Int. J. Solids Structures, 1976, Vol. 12, pp. 491–500. Pergamon Press. Printed in Great Britain

PLANE STRESS ANALYSIS OF A SCARF JOINT

THEIN WAH

Texas A and I University, Kingsville, TX 78363, U.S.A.

(*Received* 31 *July* 1975; *revised* 22 *December* 1975)

Abstract—The stress distribution in a scarf joint, with arbitrary angle of scarf, is analyzed as a two dimensional elasticity problem in plane stress. Both the adherend and the adhesive are assumed to be elastic and isotropic. The two adherends may have differing moduli of elasticity. Numerical results are given.

INTRODUCTION

With the increasing use of cemented joints in structural components[1, 2], the distribution of stresses at the adherend-adhesive interface of a scarf joint has become of importance in design.

While cemented joints other than the scarf have received wide attention for both isotropic and anisotropic materials[3–6] the only paper, known to the author, which specifically aimed at elucidating the scarf joint problem is that by J. L. Lubkin[7], wherein the author, using an elegant proof based on the semiinverse method, showed that the stresses were constant along the joint for all scarf angles provided the adherends had the same elastic properties. He also deduced the value of the single angle of scarf which would result in a state of homogeneous deformation of the cement if the elastic constants of the adherends were different.

In this paper we have attempted to give a solution of the problem for adherends having differing elastic constants.

It is believed that the solution is sufficiently accurate for design purposes provided the scarf angle is not too small.

FORMULATION OF THE PROBLEM

The scarf joint is shown schematically in Fig. 1. The forces P are assumed to be applied at some distance from the scarf, and the cement is considered to have a very small thickness t compared to the length c of the joint.

The problem is to determine the stress distribution in the cement and adjacent adherend material.

The boundary conditions for the adherends are that the top and bottom surfaces be traction free, and that the stress resultant equal P on the vertical sides. This is achieved by the use of eigenfunctions with undetermined constant coefficients.

These constants are determined by imposing two sets of conditions; first, that the stresses at the adherend-adhesive interfaces satisfy the equations of equilibrium of the adhesive treated as being very thin, and, second, that the displacements of the adhesive and adherends be compatible on the same interfaces.

The scarf angle α is arbitrary and plane stress is assumed. The materials of both the adhesive and adherends are linear-elastic, but the two adherends may have different elastic constants.

STRESS FUNCTION

We use two coordinate systems (r, θ) and (x, y) as shown in Fig. 2.

The stress function

$$\phi = \phi_1 + \phi_2 \tag{1}$$

where

$$\phi_1 = A_0 r^2(\cos 2\theta - 1) \equiv -2A_0 y^2 \tag{2}$$

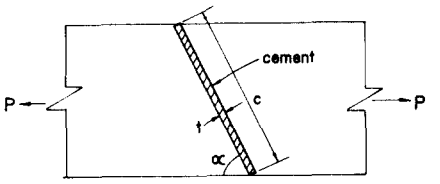

Fig. 1. Scarf joint.

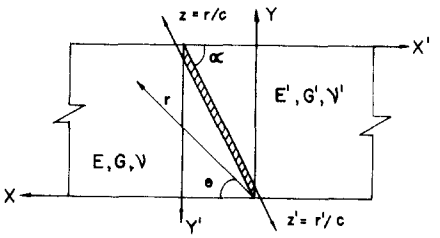

Fig. 2. Coordinates.

and

$$\phi_2 = A_1 c^2 \exp\left(\frac{-2\gamma x}{c \sin\alpha}\right)\left\{\kappa \cos\gamma\left(\frac{2y}{c\sin\alpha}-1\right)+\gamma\left(\frac{2y}{c\sin\alpha}-1\right)\sin\gamma\left(\frac{2y}{c\sin\alpha}-1\right)\right\} \tag{3}$$

is biharmonic. (A_0, A_1, and κ are constants.)

The stress components may be calculated from the relations

$$\sigma_r = \frac{1}{r}\frac{\partial\phi}{\partial r}+\frac{1}{r^2}\frac{\partial^2\phi}{\partial\theta^2}, \quad \sigma_\theta = \frac{\partial^2\phi}{\partial r^2}, \quad \tau_{r\theta} = -\frac{\partial}{\partial r}\left(\frac{1}{r}\frac{\partial\phi}{\partial\theta}\right) \tag{4}$$

$$\text{or from } \sigma_x = \partial^2\phi/\partial y^2,\ \sigma_y = \partial^2\phi/\partial x^2,\ \tau_{xy} = -\partial^2\phi/\partial x\partial y. \tag{5}$$

From equations (2) and (5) it is easily seen that the stress function ϕ_1 satisfies the boundary conditions

$$\sigma_y = \tau_{xy} = 0 \quad \text{at} \quad y = 0, c\sin\alpha \tag{6}$$

and yields also

$$\sigma_x = -4A_0,\ A_0 = -\sigma_0/4,\ \sigma_0 = P/c\sin\alpha. \tag{7}$$

The stress function ϕ_2 (eqn (3)) not only satisfies the boundary conditions at $y = 0$ and $y = c\sin\alpha$, but gives zero resultant force and couple on any section x = constant, provided γ is taken as one of the roots of the equation[8]

$$\sin 2\gamma + 2\gamma = 0 \tag{8}$$

and κ in eqn (3) is taken to be equal to $-\gamma\sin\gamma/\cos\gamma$.

Equation (8) has complex roots, which occur in conjugate pairs. Choice of only those roots which have a positive real part ensures the satisfaction of the boundary conditions at large values of $x > 0$.

The normal and shear stresses, σ_θ and $\tau_{r\theta}$ along the cement line $\theta = \alpha$, may be obtained by first calculating σ_x, σ_y and τ_{xy} from eqns (5) and then transforming to the (r, θ) system. The result is

$$\sigma_\theta = 4A_1(\gamma^2/\sin^2\alpha)X1(z, 2\alpha) + \sigma_0\sin^2\alpha \tag{9}$$

$$\tau_{r\theta} = 4A_1(\gamma^2/\sin^2\alpha)X2(z, 2\alpha) - \sigma_0\sin\alpha\cos\alpha \tag{10}$$

where the functions $X1$ and $X2$ are defined in the Appendix and the coordinate $z = r/c$ is indicated in Fig. 2.

Using Hooke's Law one may also derive expressions for the displacement components in the x and y directions and from these obtain the radial and tangential components from the formulas

$$u_r = u_x\cos\theta + v_y\sin\theta, \quad v_\theta = -u_x\sin\theta + v_y\cos\theta \tag{11}$$

The displacements u_r and v_θ along $\theta = \alpha$ may be written as follows

$$u_r = \frac{c}{2G}\frac{2\gamma}{\sin\alpha}A_1X4(z, \alpha, \nu) - \frac{c}{2G}\sigma_0\left(\sin^2\alpha - \frac{1}{1+\nu}\right)z + V\sin\alpha + H\cos\alpha \tag{12}$$

$$v_\theta = \frac{c}{2G}\frac{2\gamma}{\sin\alpha}A_1X3(z, \alpha, \nu) - \frac{c}{2G}\sigma_0 z\sin\alpha\cos\alpha - H\sin\alpha + V\cos\alpha + cRz. \tag{13}$$

In these equations, G is the shear modulus of the adherend and ν is Poisson's ratio. The constants H, V, and R define the displacements and rotation of the adherend as a rigid body. The functions $X4$ and $X3$ are defined in the Appendix.

Equations (9), (10), (12) and (13) represent the stresses and displacements of the left hand adherend in Fig. 1. A similar set of equations may be written for the right hand adherend by replacing A_1 by A_1', z by $z' = 1 - z$, G by G', ν by ν', and V, H, and R by V', H' and R'. σ_0, c and γ remain the same for the two adherends.

EQUATIONS OF EQUILIBRIUM FOR ADHESIVE

The two equations of equilibrium for the adhesive are (Fig. 3)

$$\partial\sigma_\theta/\partial n = -\partial\tau_{r\theta}/c\partial z, \quad \partial\sigma_z/c\partial z = -\partial\tau_{r\theta}/\partial n. \tag{14}$$

Since we assume the adhesive to be very thin we may replace the first of the preceding equations by

$$(\sigma_\theta' - \sigma_\theta)/t = -\partial\tau_{r\theta}/c\partial z \quad \text{and} \quad (\sigma_\theta - \sigma_\theta')/t = -\partial\tau_{r\theta}'/c\partial z'. \tag{15}$$

Adding these two equations, we get

$$\partial\tau_{r\theta}/\partial z + \partial\tau_{r'\theta}/\partial z' = 0. \tag{16}$$

From the second of (14) we may similarly derive

$$\partial\sigma_z/\partial z + \partial\sigma_z'/\partial z' = 0. \tag{17}$$

The compatibility equation

$$\frac{\partial^2\epsilon_z}{\partial n^2} + \frac{1}{c^2}\frac{\partial^2\epsilon_n}{\partial z^2} = \frac{1}{c}\frac{\partial^2(\gamma_{zn})}{\partial z\partial n}$$

is automatically satisfied if we assume $\partial^2/\partial n^2 \simeq 0$ since

$$\frac{\partial^2\epsilon_n}{\partial z^2} = \frac{\partial^2}{\partial z^2}\left(\frac{\partial v}{\partial n}\right)$$

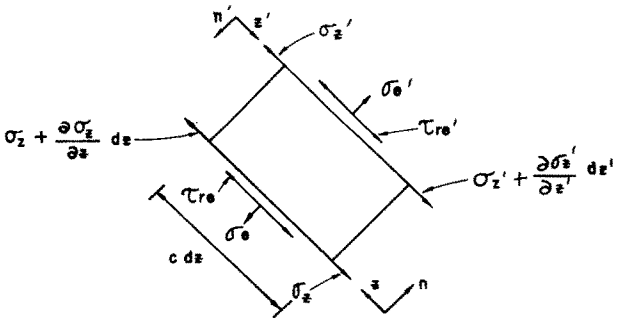

Fig. 3. Equilibrium of cement.

and

$$\frac{\partial^2}{\partial z \partial n}\gamma_{zn} = \frac{\partial^2}{\partial z \partial n}\left(\frac{\partial u}{\partial n} + \frac{1}{c}\frac{\partial v}{\partial z}\right) \simeq \frac{1}{c}\frac{\partial^2}{\partial z^2}\frac{\partial v}{\partial n}.$$

Now

$$\epsilon_z = \sigma_z/E_c - \nu_c\sigma_\theta/E_c \tag{18}$$

where E_c and ν_c are the elastic modulus and Poisson's ratio for the adhesive.

Setting $\epsilon_z = \partial u_r/c\partial z$ eqn (18) gives

$$\sigma_z = E_c\partial u_r/c\partial z + \nu_c\sigma_\theta. \tag{19}$$

Similarly,

$$\sigma'_z = E_c\partial u'_r/c\partial z' + \nu_c\sigma'_\theta. \tag{20}$$

From (19) and (20) we obtain

$$\frac{\partial\sigma_z}{\partial z} + \frac{\partial\sigma'_z}{\partial z'} = \frac{E_c}{2c}\left(\frac{\partial^2 u_r}{\partial z^2} + \frac{\partial^2 u'_r}{\partial z'^2}\right) + \frac{\nu_c}{2}\left(\frac{\partial\sigma_\theta}{\partial z} + \frac{\partial\sigma'_\theta}{\partial z'}\right). \tag{21}$$

From eqns (17) and (21) we get

$$\frac{E_c}{2c}\left(\frac{\partial^2 u_r}{\partial z^2} + \frac{\partial^2 u'_r}{\partial z'^2}\right) + \frac{\nu_c}{2}\left(\frac{\partial\sigma_\theta}{\partial z} + \frac{\partial\sigma'_\theta}{\partial z'}\right) = 0. \tag{22}$$

Equations (16) and (22) are the two equations of equilibrium for the adhesive.

EQUATIONS OF COMPATIBILITY

Approximately, the shear strains on the two surfaces of the adhesive are

$$\gamma_{r\theta} = -(u_r + u'_r)/t + \partial v_\theta/c\partial z$$

and

$$\gamma_{r'\theta} = -(u_r + u'_r)/t + \partial v'_\theta/c\partial z'.$$

Using Hooke's Law we get

$$u_r + u'_r = -(t/2G_c)(\tau_{r\theta} + \tau'_{r\theta}) + (t/2c)(\partial v_\theta/\partial z + \partial v'_\theta/\partial z') \tag{23}$$

and also

$$v_\theta + v_{\theta'} = -(t/2E_c)[\sigma_\theta + \sigma_{\theta'} - \nu_c(\sigma_z + \sigma'_z)] \tag{24}$$

where G_c is the shear modulus of the adhesive.

Substituting from (19) and (20) into (24), the latter becomes

$$v_\theta + v_{\theta'} = -(t/2E_c)[(1-\nu_c^2)(\sigma_\theta + \sigma'_\theta) - (\nu_c E_c/c)(\partial u_r/\partial z + \partial u'_r/\partial z')]. \tag{25}$$

Reference to eqns (12) and (13) shows that eqns (23) and (25) contain the rigid body terms H, V, Rz and H', V' and $R'(1-z)$. These terms are eliminated by differentiating (23) once and (25) twice with respect to z. Equations (23) and (25) then take the form

$$\partial u_r/\partial z - \partial u'_r/\partial z' + (t/2G_c)(\partial\tau_{r\theta}/\partial z - \partial\tau'_{r\theta}/\partial z') - (t/2c)(\partial^2 v_\theta/\partial z^2 - \partial^2 v'_\theta/\partial z'^2) = 0 \tag{26}$$

$$\partial^2 v_\theta/\partial z^2 + \partial^2 v'_\theta/\partial z'^2 + (t(1-\nu_c^2)/2E_c)(\partial^2\sigma_\theta/\partial z^2 + \partial^2\sigma'_\theta/\partial z'^2) - (\nu_c t/2c)(\partial^3 u_r/\partial z^3 + \partial^3 u'_r/\partial z'^3) = 0. \tag{27}$$

The stress and displacement components given by eqns (9)–(13) and similar equations for the right hand adherend are now substituted into eqns (15), (22), (26) and (27). The resulting equations

may be written as follows:

$$A_1 Q_1(z, \gamma, 2\alpha) + A_1' Q_1(z', \gamma, 2\alpha) = 0 \tag{28}$$

$$A_1 Q_2(z, \gamma, \alpha, \nu, 1) + A_1' Q_2(z', \gamma, \alpha, \nu', \mu) = 0 \tag{29}$$

$$A_1 Q_3(z, \gamma, \alpha, \nu, 1) - A_1' Q_3(z', \gamma, \alpha, \nu', \mu) = 0.25\sigma_0 \sin\alpha\{\sin^2\alpha - 1/1 + \nu - \mu(\sin^2\alpha - 1/1 + \nu')\} \tag{30}$$

$$A_1 Q_4(z, \gamma, \alpha, \nu, 1) + A_1' Q_4(z', \gamma, \alpha, \nu', \mu) = 0 \tag{31}$$

in which $\mu = G/G'$ is the stiffness ratio of the adherends, and the Q_i are given in the Appendix.

It should be remarked that the set of eqns (28)–(31) (and all preceding equations) are presented in abbreviated form. A_1 and A_1' are complex constants since γ is a complex number. The complex conjugate of γ, must also be included in the equations, and therefore also the complex conjugates of A_1 and A_1'. Thus, if only a single root of eqn (8) is used, we have four unknown constants in each equation.

Before proceeding to a description of the method of solution used, we remark that the basic eqns (28)–(31) are all homogeneous with the exception of eqn (30). If the right hand member of (30) vanishes we obtain a set of homogeneous equations with the trival solution $A_1 = A_1' = 0$. This will occur if the elastic constants of the two adherends are identical, i.e.

$$\mu = 1, \quad \nu = \nu' \tag{32}$$

or when

$$\sin^2\alpha - 1/1 + \nu = \mu(\sin^2\alpha - 1/1 + \nu'). \tag{33}$$

Equation (33), with the necessary change in notation, leads to the single value of α for which we obtain constant adhesive stresses for unequal adherends as pointed out by Lubkin.[7]

SOLUTION OF EQUATIONS

The method used for solving the equations is point matching. We have generally used the first 5 of the following 10 roots of eqn (8)

$$\begin{aligned} \gamma_{1,2,3,4,5} &= 2.1061 \pm i\,1.1254,\ 5.3563 \pm i\,1.5516, \\ &\quad 8.5367 \pm i\,1.7755,\ 11.6992 \pm i\,1.9294, \\ &\quad 14.5841 \pm i\,2.0469 \\ \gamma_{6,7,8,9,10} &= 18.0049 \pm i\,2.1419,\ 21.1534 \pm i\,2.2217, \\ &\quad 24.3003 \pm i \cdot 2.2906,\ 27.4462 \pm i\,2.3510, \\ &\quad 30.5913 \pm i\,2.4050 \end{aligned} \tag{34}$$

so that there are 20 unknown constants in each of the equations. The equations are satisfied at 11 points $z = 0, 0.1, \ldots, 1$, resulting in a total of 44 equations in 20 unknowns. A linear least squares procedure is then used to obtain the 20 unknown constants.

The stresses σ_θ, $\tau_{r\theta}$, $\sigma_{\theta'}$, $\tau_{r\theta'}$ and the average longitudinal stress $\bar{\sigma}z = (\sigma_z + \bar{\sigma}_z)/2$ are then calculated. The equation for $\bar{\sigma}z$ is given in the Appendix.

NUMERICAL RESULTS AND CONCLUSIONS

Figures 4–8 give the numerical results obtained for the normal and shear stress and Table 1 the stress $\bar{\sigma}_z$ along the adhesive, for various scarf angles α varying from 90° to 60° and for several values of the stiffness ratio μ. We have assumed the Poisson's ratio for both the adherends to be 0.3. Other parameters were arbitrarily chosen taking care only to keep the t/c ratio small for the adhesive. The following numerical values were used in the calculations:

$$\lambda_1 = Gt/G_c c = 0.1, \quad \lambda_2 = Gt/E_c c = \lambda_1/2.5, \quad \lambda_3 = \nu_c t/2c = 0.000125$$
$$\lambda_4 = \lambda_3/\lambda_2\nu_c^2, \quad \lambda_5 = \lambda_3/\nu_c, \quad \nu_c = 0.25, \quad \mu = 0.5, 0.1, 0.01.$$

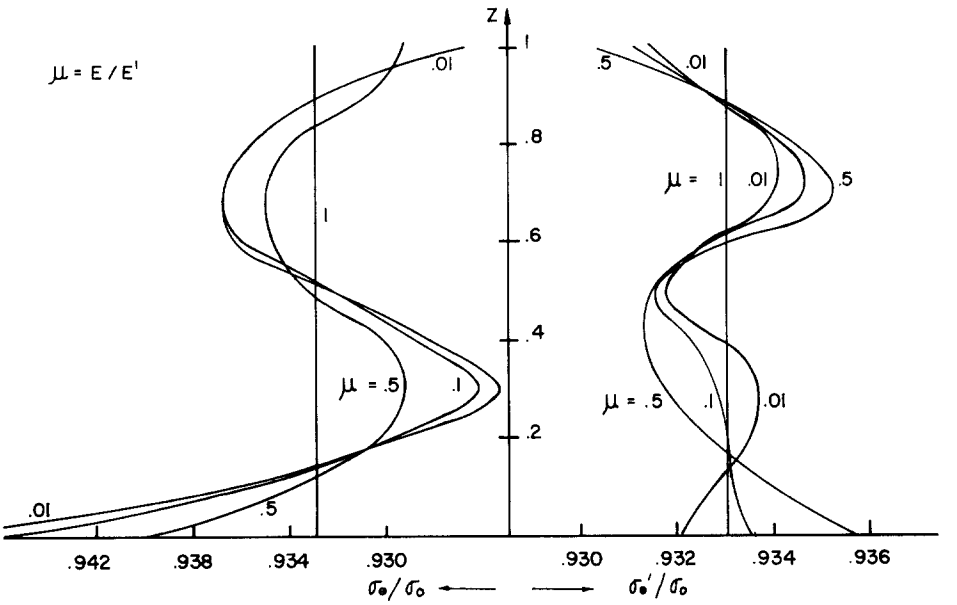

Fig. 4. $\alpha = 75°$ normal stresses.

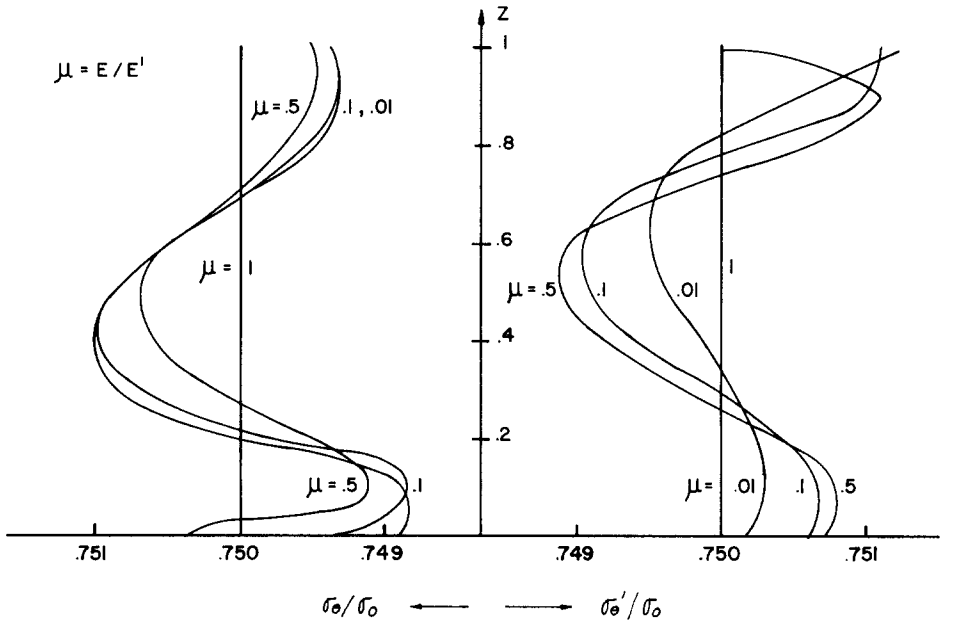

Fig. 5. $\alpha = 60°$ normal stresses.

We remark that the plane strain problem which more nearly approaches the practical case, may be obtained from the present problem by substituting $E/(1-\nu^2)$ for E and $\nu/(1-\nu)$ for ν wherever these quantities occur.

Several remarks are in order regarding the probable limitations of the present analysis. While, intuitively, one would assume that the accuracy of the solution will increase with the number of roots employed, there are severe practical limitations to the procedure. The higher roots (see eqns 34) involve exponentials with a very large negative real part and the computed figures become quite meaningless after about the seventh root. The situation is aggravated for small scarf angles because the values of the exponentials decrease rapidly within the scarf. For small scarf angles (of the order of 15°), it might be necessary to use fewer than 5 roots to obtain reliable figures. However this is not entirely a matter of the scarf angle, but depends, although to a lesser extent, on other parameters such as relative stiffness of cement and adherends.

Thus far, the author has not found it possible to generate good results using 10 roots and has

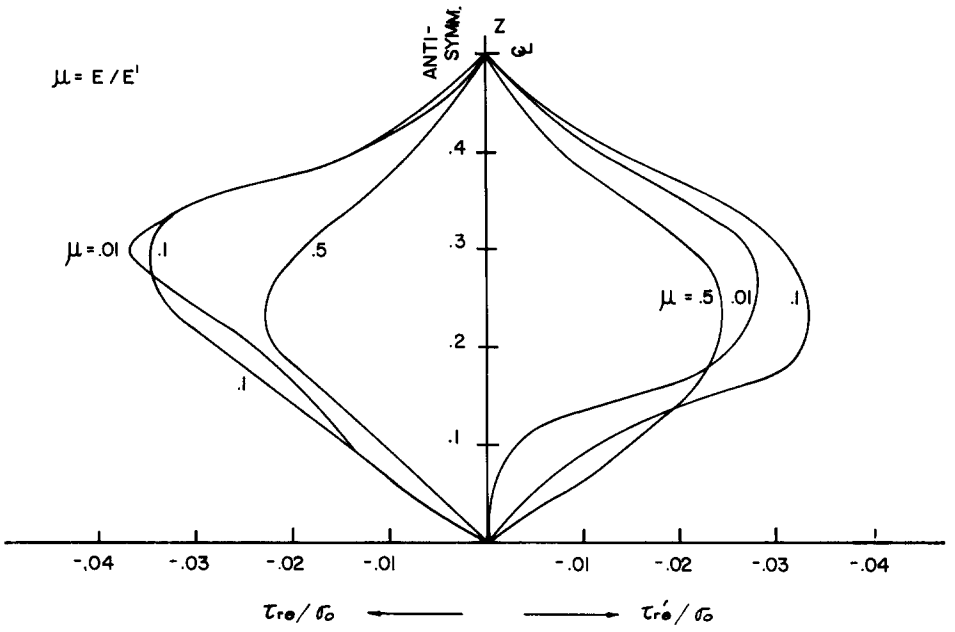

Fig. 6. $\alpha = 90°$ shear stresses.

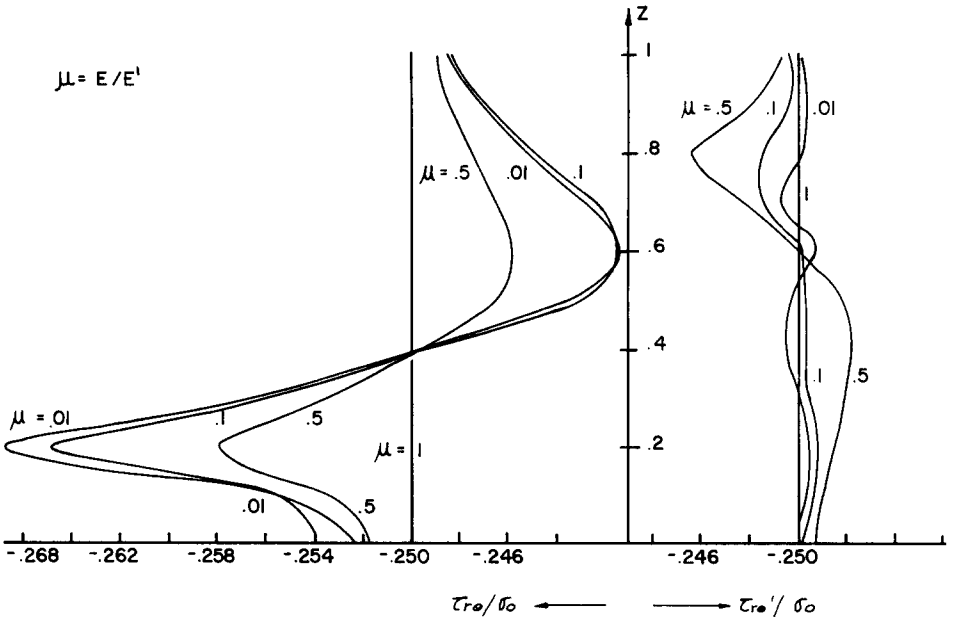

Fig. 7. $\alpha = 75°$ shear stresses.

listed the higher roots primarily to indicate their relative magnitudes. For 7 roots the results were mixed. Some of the solutions were obviously unacceptable, while those that converged gave results virtually identical with those for the 5 root scheme, at least for normal and shear stresses. Noticeable changes were found only in the axial stress ($\bar{\sigma}_z$) in the cement. Some comparative figures for this are given in Table 1. It is necessary to add, however, that convergence, in the sense of the diminution of the coefficients A_i with increase of i, was best when 5 roots were used.

From the pattern of normal and shear stress distribution, as seen from Figs. 4 to 8, there are only a few general conclusions that can be drawn. First, the distribution of stresses are quite different on the two sides of the cement, one having no similarity to the other. The stresses fluctuate about the "average stress" (that corresponding to $\mu = 1$), but in a manner in which no regular pattern can be discerned.

The computed data show rapid fluctuations in the magnitude of the normal and shear stresses

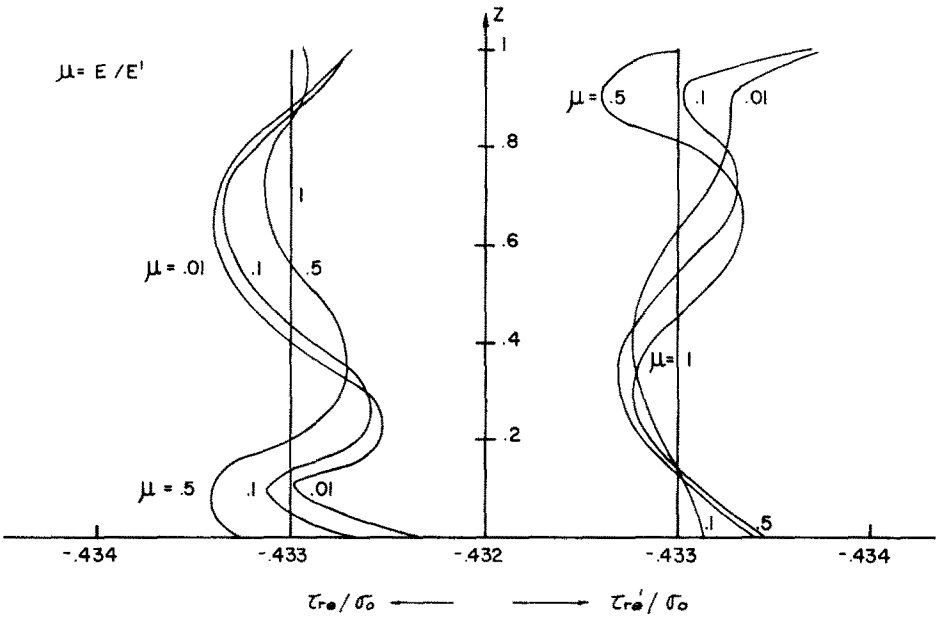

Fig. 8.

Table 1. Average values of $\bar{\sigma}_z/\sigma_0$

μ \ Scarf Angle	90°	75°	60°
1	0.247	0.2313	0.188
0.5	1.25	1.16	0.983
		(1.63)†	(1.31)
0.1	1.25	1.17	0.983
		(1.63)	(1.31)
0.01	1.25	1.17	0.938
		(1.63)	(1.31)

†Figures in parentheses were obtained using 7 roots. Except of $\mu = 1$, other figures represent results with 5 roots.

over the length of the joint. Some of these fluctuations must be discounted, for it is to be remembered that the stresses are computed using coefficients obtained by a least squares fit, and while the overall picture of the stress distribution may be accurate enough, local inaccuracies are to be expected.

Despite the apparent fluctuations, however, an examination of the scale to which the curves are drawn will show that for all scarf angles the fluctuations from the uniform distribution (for $\mu = 1$) are negligibly small. Indeed, we have had to omit showing the normal stresses for the 90° scarf because the stress distribution did not deviate sufficiently from uniformity to be shown on a graph. For the other scarf angles the deviations are more pronounced. But it may be noted that in Fig. 7 which shows apparently large fluctuations, the maximum deviation from the uniform stress is less than 7%, even though the adherend stiffnesses ratios vary from 0.5 to 0.01. Of course, an exception to this general statement is the shear stress distribution in the 90° scarf, which is zero for $\mu = 1$.

It might seem that in our examples the stiffness of the glue is small compared to that of either adherend and if this ratio is changed a different stress picture might emerge. As a matter of fact, many other ratios (and many smaller scarf angles) were tried, without radically altering the near overall uniformity of the stress distribution. (There were, of course, changes in detail.) Nevertheless the author considers it possible that there could be a combination of parameters that would make the distribution very different.

The difference in elastic constants of the adherends does, however, have a marked effect on the longitudinal stress $\bar{\sigma}_z$ on the cement as can be seen from Table 1. $\bar{\sigma}_z$ is only the "average" longitudinal stress so that the maximum stress, adjacent to the stiffer adherend, will be greater. The longitudinal stress is also almost constant along the adhesive although it might well turn out to be the critical stress in design.

The numerical data presented here are too limited in scope to justify more general conclusions. The parameters involved in the problem are many, and the range of parameters will depend on the type of application contemplated.

REFERENCES

1. R. L. Patrick, (Editor), *Treatise on Adhesion and Adhesives*, Vol. 3. Marcel Dekker, New York (1973).
2. G. Lubin (Editor), *Handbook of Fiberglass and Advanced Plastics Composites*. Van Nostrand, New York (1964).
3. M. Goland and E. Reisner, Stresses in Cemented Joints. *J. Appl. Mech.* **11**, A17 (1944).
4. F. Szepe, Strength of adhesive-bonded lap joints with respect to change of temperature and fatigue, *Experi. Mechan.* **6**, 281 (1966).
5. O. Volkersen, Die Nietraftverteilung in Zugbeanspruchten Nietverbindungen mit Konstanten Laschenquerschnitten. *Luftfahrtforschung*, **15**, 41 (1938).
6. Thein Wah, Stress distribution in a bonded anisotropic lap joint, *J. Mater. Tech.* 174 (1973).
7. J. L. Lubkin, A Theory of Adhesive Scarf Joints, *J. Appl. Mech.* **24**, 255 (1957).
8. S. Timoshenko and J. N. Goodier, *Theory of Elasticity*. 3rd Edn, pp. 61–62. McGraw-Hill, New York (1970).

APPENDIX

$$H = \exp(-2\gamma z \cot\alpha)$$

$$F_1(z,\alpha) = \sin\{\gamma(2z-1)-\alpha\} \tag{A1}$$

$$F_2(z,\alpha) = \cos\{\gamma(2z-1)-\alpha\} \tag{A2}$$

$$F_3(z,\alpha) = \gamma(2z-1)\sin\{\gamma(2z-1)-\alpha\} \tag{A3}$$

$$F_4(z,\alpha) = \gamma(2z-1)\cos\{\gamma(2z-1)-\alpha\} \tag{A4}$$

$$X1(z,2\alpha) = [F_2(z,2\alpha)(\kappa-1) + F_3(z,2\alpha) + F_2(z,0)]H \tag{A5}$$

$$X2(z,2\alpha) = [F_1(z,2\alpha)(1-\kappa) + F_4(z,2\alpha)]H \tag{A6}$$

$$X3(z,\alpha,\nu) = [F_1(z,\alpha)(\kappa - 2\nu/(1+\nu)) - F_4(z,\alpha) + 2(1-\nu)F_2(z,0)\sin\alpha/1+\nu + F_1(z,0)\cos\alpha]H \tag{A7}$$

$$X4(z,\alpha,\nu) = [F_2(z,\alpha)(\kappa - 2\nu/(1+\nu)) + F_3(z,\alpha) - 2(1-\nu)F_2(z,0)\cos\alpha/1+\nu + F_1(z,0)\sin\alpha]H \tag{A8}$$

In the following equations the function F_1, F_2, F_3, and F_4 on the right hand side have the same argument for α as shown on the left hand side, unless otherwise indicated.

$$DX1(z,2\alpha) = [F_1(2-\kappa) - \cot\alpha F_2(1+\kappa) - \cot\alpha F_3 + F_4 + F_1(z,0) + \cot\alpha F_2(z,0)]H \tag{A9}$$

$$DX2(z,2\alpha) = [\cot\alpha F_1(\kappa-1) + F_2(2-\kappa) - F_3 - \cot\alpha F_4]H \tag{A10}$$

$$DX3(z,\alpha,\nu) = [\cot\alpha F_1(2\nu/(1+\nu)-\kappa) + F_2(\kappa - 2\nu/(1+\nu) - 1) + F_3 + F_4\cot\alpha - 2(1-\nu)\sin\alpha\{F_1(z,0) + \cot\alpha F_4(z,0)\}/1+\nu + \{F_2(z,0) - \cot\alpha F_1(z,0)\}\cos\alpha]H \tag{A11}$$

$$DX4(z,\alpha,\nu) = [F_1(1 + 2\nu/(1+\nu) - \kappa) + \cot\alpha F_2(\kappa - 2\nu/1+\nu) + F_4 - \cot\alpha F_3 + 2(1-\nu)\cos\alpha\{F_1(z,0) - \cot\alpha F_2(z,0)\}/(1+\nu) + \{F_2(z,0) - \cot\alpha F_1(z,0)\}\sin\alpha]H \tag{A12}$$

$$DDX1(z,2\alpha) = [2\cot\alpha\{F_1(\kappa-2) - F_4 + F_1(z,0)\} + F_2\{\kappa(\cot^2\alpha - 1) + 2\} + (\cot^2\alpha - 1)\{F_2(z,0) + F_3\}]H \tag{A13}$$

$$DDX3(z,\alpha,\nu) = [F_1\{(\cot^2\alpha - 1)(\kappa - 2\nu/(1+\nu)) + 2\} + 4F_1(z,0)\cos\alpha(1-\nu)/(1+\nu) + 2F_2\cot\alpha(1 - \kappa + 2\nu/1+\nu) + 2F_2(z,0)(\cot^2\alpha - 1)\sin\alpha(1-\nu)/(1+\nu) - 2\cot\alpha F_3 - (\cot^2\alpha - 1)F_4 + \cos\alpha\{F_1(z,0)(\cot^2\alpha - 1) - 2\cot\alpha F_2(z,0)\}]H \tag{A14}$$

$$DDX4(z,\alpha,\nu) = [2\cot\alpha F_1(\kappa - 1 - 2\nu/(1+\nu)) + F_2(\cot^2\alpha - 1)(\kappa - 2\nu/(1+\nu)) + (\cot^2\alpha - 1)F_3 - 2\cot\alpha F_4 - 2(1-\nu)\cos\alpha\{F_2(z,0)(\cot^2\alpha - 1) + 2\cot\alpha F_1(z,0)\}/(1+\nu) + \sin\alpha\{F_1(z,0)(\cot^2\alpha - 1) - 2\cot\alpha F_2(z,0)\}]H \tag{A15}$$

$$DDDX4(z,\alpha,\nu) = [F_1\{(3\cot^2\alpha - 1)(1 - \kappa + 2\nu/(1+\nu)) - 2\} + F_2\cot\alpha\{(3 - \cot^2\alpha)(\kappa - 2\nu/(1+\nu)) - 6\} + F_3\cot\alpha(3 - \cot^2\alpha) + F_4(3\cot^2\alpha - 1) + 2F_1(z,0)(1-\nu)\cos\alpha(3\cot^2\alpha - 1)/(1+\nu) - 2F_2(z,0)(1-\nu)\cos\alpha\cot\alpha(3 - \cot^2\alpha)/(1+\nu) + \{F_2(z,0)(3\cot^2\alpha - 1) + F_1(z,0)\cot\alpha(3 - \cot^2\alpha)\}\sin\alpha]H \tag{A16}$$

$$Q_1(z,\gamma,2\alpha) = \gamma^3 DX2(z,2\alpha) \tag{A17}$$

$$Q_2(z,\gamma,\alpha,\nu,T) = \gamma^3[\sin\alpha\lambda_4 TDDX4(z,\alpha,\nu) + DX1(z,2\alpha)] \tag{A18}$$

$$Q_3(z,\gamma,\alpha,\nu,T) = \gamma^2[TDX4(z,\alpha,\nu) + 2\gamma\lambda_1 DX2(z,2\alpha)/\sin\alpha - 2\gamma\lambda_5 TDDX3(z,\alpha,\nu)] \tag{A19}$$

$$Q_4(z, \gamma, \alpha, \nu, T) = \gamma^3[T \sin \alpha DDX3(z, \alpha, \nu) + 2\gamma\lambda_2(1 - \nu_c^2)DDX1(z, 2\alpha) - 2T\gamma\lambda_3 \sin \alpha DDDX4(z, \alpha, \nu)] \tag{A20}$$

$$\bar{\sigma}z = COF*4\gamma^2 \operatorname{cosec} \alpha[A_1 DX4(z, \alpha, \nu) + A_1'\mu DX4(z', \alpha, \nu')] + 0.5\nu_c(\sigma_\theta + \sigma_{\theta'}) - \sigma_0 COF[\sin^2 \alpha - 1/(1 + \nu) + \mu(\sin^2 \alpha - 1/(1 + \nu'))] \tag{A21}$$

$$COF = \lambda_3/2\nu_c\lambda_2 \tag{A22}$$

$$\kappa = -\gamma \sin \gamma/\cos \gamma. \tag{A23}$$